Dislocated tongue muscle attachment connected to cleft palate formation

T. Kouskoura[1]*, Y. El Fersioui[1]*, M. Angelini[1], D. Graf[2], C. Katsaros[1], and M. Chiquet[1]

J Dent Res. 2015 Dec 23. pii: 0022034515621869. [Epub ahead of print]

Dislocated tongue muscle attachment connected to cleft palate formation

T. Kouskoura[1]*, Y. El Fersioui[1]*, M. Angelini[1], D. Graf[2], C. Katsaros[1], and M. Chiquet[1]

[1]Department of Orthodontics and Dentofacial Orthopedics, School of Dental Medicine, University of Bern, Bern, Switzerland
[2]School of Dentistry, Faculty of Medicine & Dentistry, University of Alberta, Edmonton, Canada

* These authors contributed equally to the work.

Corresponding author:
M. Chiquet, PhD
Department of Orthodontics and Dentofacial Orthopedics
School of Dental Medicine
University of Bern
Freiburgstrasse 7
CH-3010 Bern, Switzerland
Email: matthias.chiquet@zmk.unibe.ch
Phone: +41 31 632 9882
Fax: +41 31 632 9869

Abstract

In Pierre Robin sequence, a retracted tongue due to micrognathia is thought to physically obstruct palatal shelf elevation and thereby cause cleft palate. However, micrognathia is not always associated with palatal clefting. Here, by using the *Bmp7*-null mouse model presenting with cleft palate and severe micrognathia, we provide the first causative mechanism linking the two. In wildtype embryos the genioglossus muscle, which mediates tongue protrusion, originates from the rostral process of Meckel's cartilage and later from the mandibular symphysis, with two tendons positive for *Scleraxis* mRNA. In E13.5 *Bmp7*-null embryos, a rostral process failed to form, and a mandibular symphysis was absent at E17.5. Consequently, the genioglossus muscle fibers were diverted towards the lingual surface of Meckel's cartilage and mandibles, where they attached in an aponeurosis that ectopically expressed *Scleraxis*. The deflection of genioglossus fibers from the anterior-posterior towards the medial-lateral axis alters their direction of contraction and necessarily compromises tongue protrusion. Since this muscle abnormality precedes palatal shelf elevation, it is likely to contribute to clefting. In contrast, embryos with a cranial mesenchyme-specific deletion of *Bmp7* (*Bmp7*:Wnt1-Cre) exhibited some degree of micrognathia, but no cleft palate. In these embryos a rostral process was present, indicating that mesenchyme-derived Bmp7 is dispensable for its formation. Moreover, the genioglossus appeared normal in *Bmp7*:Wnt1-Cre embryos, further supporting a role of aberrant tongue muscle attachment in palatal clefting. We thus propose that in Pierre Robin sequence, palatal shelf elevation is not impaired simply by physical obstruction by the tongue, but by a specific developmental defect that leads to functional changes in tongue movements.

Key words:

Bone morphogenetic protein 7; Pierre Robin sequence; micrognathism; glossoptosis; cartilage; mandible

Introduction

Recent evidence suggests that mutations in the gene for Bone Morphogenetic Protein 7 (BMP7) in humans disturb the formation of the secondary palate during embryogenesis and result in cleft palate (Wyatt et al. 2010; Yu et al. 2015). We previously reported on a *Bmp7*-null mouse model with cleft of the secondary palate as part of a syndromic phenotype resembling Pierre Robin sequence, which includes severe micrognathia (Kouskoura et al., 2013). A recent review has identified a number of studies on mouse models that exhibit features of micrognathia, glossoptosis (retraction of the tongue), and cleft palate (Price et al. 2015), some with striking similarity to our model (Murray et al. 2007; Warner et al. 2013; Iwata et al. 2015). However, how the lack of Bmp7 eventually leads to cleft palate remains unknown.

A cause and effect relationship between micrognathia/retrognathia and clefting of the secondary palate is not universally accepted. The hypothesis implicating micrognathia or retrognathia in palatal clefting assumes that a rapid withdrawal of the tongue is required at a critical stage of palatogenesis to allow the elevation and approximation of the palatal shelves at the midline (Price et al. 2015). At such an early developmental stage (E14-E14.5 in mouse embryos), the only mature skeletal structure in the mandibular process is Meckel`s cartilage, which is thought to act as the template around which incompletely known signalling mechanisms lead to growth of the mandibular bone (Sugito et al. 2011). A direct implication of different Bmps (including Bmp7) in early formation of Meckel`s cartilage was shown by using Bmp-soaked beads as sources of signaling towards mandibular mesenchyme from chick or mouse embryos (Nonaka et al. 1999; Mina et al. 2002). When applied to early mandibular processes, Bmps induced the expression of transcription factor Sox9, which initiated chondrogenesis and appearance of Meckel`s cartilage. Earlier studies in rat and mouse embryos have shown an increase in size of Meckel`s cartilage preceeding palatal shelf elevation, and the deterioration of this transient structure after that (Diewert 1980; Luke 1989). This suggested a link between the strengthening of Meckel`s cartilage and its proposed function in supporting early tongue movements. Anatomical studies in human embryos (Lee and Saint-Jeannet 2011) showed that at the stage of palatal shelf elevation, the genioglossus muscle is indeed attached to the rostral process of Meckel`s cartilage and could mediate protrusion and lowering of the tongue.

Since we could not detect any obvious defects in proliferation and growth of the palatal shelves and in their ability to fuse *in vitro* in our mouse model (Kouskoura et al. 2013), we investigated how severe micrognathia might disturb palatal shelf elevation. We found that in the absence of Bmp7, an altered development and morphology of Meckel`s cartilage

causes specific displacements of the attachment sites of the genioglossus muscle, thus disturbing its function in tongue protrusion.

Materials and Methods

Animals

All experiments involving mice were approved by the Cantonal Veterinary Office of Bern, Switzerland (license No. BE88/13) or the Research Ethics Office of the University of Alberta (permit AUP000149) in accordance with the guidelines of the Canadian Council on Animal Care (CCAC). Characterization of C57BL/6 mice heterozygous for a *Bmp7* null allele has been published before (Zouvelou et al. 2009). Male and female *Bmp7* heterozygous null mice were mated to obtain $Bmp7^{+/+}$, $Bmp7^{+/\Delta}$ and $Bmp7^{\Delta/\Delta}$ embryos from the same litter. Appearance of a vaginal plug was considered embryonic day 0.5 (E0.5). Pregnant females were sacrificed by cervical dislocation at stages E12.5 -E17.5; embryos were collected and decapitated. Embryos were genotyped by allele-specific PCR (Zouvelou et al. 2009). For cranial neural crest-specific deletion a conditional *Bmp7* allele (Zouvelou et al. 2009) was crossed to wnt1-Cre (Danielian et al. 1998). The study was performed in accordance with ARRIVE guidelines; in total, 14 pregnant female mice and 110 embryos were used.

Tissue sectioning and staining

For in situ hybridization, mouse embryo heads were fixed in 4% paraformaldehyde (pH 7.5), soaked in 30% sucrose, embedded in O.C.T compound (Sakura Finetek Europe B.V., Zoeterwoude, Netherlands), frozen and stored at -80°C as described (d'Amaro et al. 2012). 12 µm thick serial frontal sections were cut on a cryomicrotome (Leica Microsystems, Heerbrugg, Switzerland), dried at 37°C, and stored at -80°C. For histological analysis, paraformaldehyde-fixed tissues were embedded in paraffin and sectioned at 5-6 µm. Sections were stained with hematoxylin and eosin (H/E), and mounted with xylene-based mounting medium.

RNA probes and in situ hybridization

Gene specific digoxygenin-labeled RNA probes were generated as published before (d'Amaro et al. 2012). Sequences of gene specific primers (Microsynth, Balgrach, Switzerland) are listed in Supplemental Table 1. Using embryonic mouse cDNA as template,

specific products were amplified by PCR and cloned into pBluescript SK+ plasmid (Stratagene/Agilent, Santa Clara, USA). Inserts were confirmed by sequencing (Microsynth), and labeled antisense RNA probes were produced with a digoxygenin labeling kit (Roche Diagnostics, Rotkreuz, Switzerland). In situ hybridization on cryosections was performed as described (Fluck et al. 2000). After incubation with alkaline phosphatase conjugated anti-digoxygenin antibody (Roche Diagnostics), a color substrate solution was used to which 10% polyvinyl alcohol (MW 31'000-50'000; Sigma-Aldrich, Buchs, Switzerland) was added (Shen, 2001). After development, the sections were counterstained with Nuclear Fast Red (Sigma).

Results

Impaired Meckel's cartilage and rostral process development in Bmp7$^{\Delta/\Delta}$ embryos

As we had shown previously, E14.5 *Bmp7*$^{\Delta/\Delta}$ embryos exhibit a delay in palatal shelf elevation, which later results in cleft palate (Kouskoura et al. 2013). However, when isolated *Bmp7*-deficient E13.5 maxillae or palatal shelves were grown in culture, shelf elevation (Supplementary Fig. 1) and fusion (Kouskoura et al. 2013) appeared to occur quite normally. Here, we therefore asked whether palatal clefting of *Bmp7*$^{\Delta/\Delta}$ embryos might be caused indirectly, e.g. by a malformed lower jaw. Indeed, at the stage of palatal shelf elevation (E14.5) these embryos present with micrognathia and unfused Meckel's cartilages (Kouskoura et al. 2013). We therefore explored at which stage a defect in Meckel's cartilage was first visible in *Bmp7*$^{\Delta/\Delta}$ embryos, and how this affected mandible and symphysis formation. By Alcian Blue staining at E12.5 (Fig. 1), left and right Meckel's cartilages extended from the future temporomandibular joint rostrally towards the midline; their anterior ends were still 1 mm apart. No obvious difference was observed between *Bmp7*$^{\Delta/\Delta}$ and wildtype embryos at this stage (Fig. 1A, B). One day later (E13.5), Meckel's cartilages had doubled in length and just met at the midline in wildtype embryos (Fig. 1C). In contrast, they were shorter and more curved in E13.5 *Bmp7*$^{\Delta/\Delta}$ embryos, and their anterior ends were still widely apart (Fig. 1D). At E14.5, Meckel's cartilages were fused in a prominent rostral process in the wildtype, but remained unfused in *Bmp7*$^{\Delta/\Delta}$ embryos (not shown; c.f. Kouskoura et al. 2013).

To explore whether anterior Meckel's cartilage and rostral process were missing in *Bmp7*$^{\Delta/\Delta}$ embryos because their primordia failed to form, or whether cartilage differentiation was impaired, we performed in situ hybridization for *Sox9* and *Col2a1*. At E12.5, an unpaired medial region of *Sox9* expression was detected at the rostral tip of the mandibular arch in both *Bmp7*$^{+/+}$ (Fig. 1E) and *Bmp7*$^{\Delta/\Delta}$ embryos (Fig. 1F), although it was weaker in the mutant.

In contrast, *Col2a1* was expressed there only in wildtype but not *Bmp7*$^{\Delta/\Delta}$ embryos (Fig. 1E, F). Thus it appears that in the absence of Bmp7, a *Sox9*-positive mesenchymal condensation is initially formed to some extent at the rostral tip of the mandibular arch, but fails to differentiate. No differences were seen between wildtype and mutant mandibular arches in cell proliferation, and no significant apoptosis was detected (not shown).

Expression of Bmp7 during mandibular arch formation

In situ hybridization of serial frontal sections through wildtype E13.5 mandibular arches revealed widespread expression of *Bmp7* mRNA (Fig. 2A-C) in epithelium, mesenchyme, and mesoderm. Expression was prominent in the basal layer of the epidermis, around incisor tooth buds, and in osteogenic areas of the mandibles. A weaker but specific signal was also detected in Meckel's cartilage and in developing tongue muscles (Fig. 2C). Although *Bmp4* shows a similar expression pattern in the mandibular arch (Fig. 2D), it obviously does not compensate for Bmp7. No hybridization was seen with a *Bmp7* sense probe (Fig. 2E), and only a very weak signal was detected with antisense probe on sections from *Bmp7*$^{\Delta/\Delta}$ embryos (Fig. 2F). Thus, *Bmp7* is expressed by several tissues of the mandibular arch (bone, cartilage, muscle), all of which are also negatively affected by its absence. This points to a largely autocrine action of *Bmp7* in these structures, rather than to a directed signaling from one tissue to another.

Lack of mandibular symphysis and mental spine formation in Bmp7$^{\Delta/\Delta}$ *embryos*

We asked next how the lack of a rostral process affected development of mandibles and symphysis at later stages. By whole mount staining, E17.5 *Bmp7*$^{\Delta/\Delta}$ lower jaws exhibited mandibular bones that were severely blunted at their anterior ends, whereas mandibular symphysis formation had started in wildtype embryos (Fig. 3A, B). Additionally, in frontal sections a cleft palate was clearly recognizable in mutant embryos (Fig. 3C, D). On most rostral sections of E17.5 wildtype embryo heads, the tips of the two mandibles were recognizable by their strong expression of *Col1a1* (collagen type I, Fig. 3E). Alveolar bone formed around the incisor tooth buds, and at the midline the mandibles touched the rostral process of Meckel's cartilage, which was negative for *Col1a1* expression (Fig. 3E). In addition, aggrecan (*Acan*)-positive, secondary symphysial cartilage could be observed left and right from the rostral process. In contrast, all these structures were absent on rostral sections of E17.5 *Bmp7*$^{\Delta/\Delta}$ embryo heads, and the incisor tooth buds were touching each other (Fig. 3F). More posteriorly, the rostral process of wildtype embryos separated into the two Meckel's cartilages, which were embedded in mandibular bone (Fig. 3G). In the cleft

between the mandibles, two *Col1a1*-positive protrusions could be observed on the bone surface. At their cranial aspect, *Acta2*-positive skeletal muscle fibers (Babai et al. 1990) were detected (Fig. 3G). Thus, these bone protrusions are likely precursors of the mandibular mental spines, from which the genioglossus muscle originates. At the same level in $Bmp7^{\Delta/\Delta}$ embryos, the tips of the more cylinder-shaped mandibles became visible; embedded Meckel's cartilage was barely recognizable (Fig. 3H). At this level, $Bmp7^{\Delta/\Delta}$ mandibles were separated by just a small cleft, in which no bone protrusions were visible. In addition, the arrangement of tongue muscle fibers was clearly aberrant (Fig. 3H; see next paragraph). Thus, E17.5 $Bmp7^{\Delta/\Delta}$ embryos lack a symphysis and associated structures at the tips of their mandibles.

Misplaced origin of genioglossus muscle in $Bmp7^{\Delta/\Delta}$ embryos

Genioglossus and the smaller geniohyoid are paired extrinsic tongue muscles that originate from the mental spines, bony projections at the mandibular symphysis. From their rostral origin, genioglossus fibers run posterior-cranially and insert into the tongue; their function is tongue protrusion.

The genioglossus muscle primordia are first observed at E12.5 as two groups of *MyoD*- and *Acta2*-expressing cells situated at the basis of the tongue left and right from the midline; no obvious differences were observed between $Bmp7^{+/+}$ and $Bmp7^{\Delta/\Delta}$ embryos at this stage (not shown). In frontal sections of E13.5 wildtype heads, muscle fibers were seen to reach out from the tongue base towards two regions on the rostral-medial surface of Meckel's cartilages, which were positive for tendon-specific transcription factor *Scx* (Scleraxis; Schweitzer et al. 2001) (Fig. 4A). In $Bmp7^{\Delta/\Delta}$ embryos of the same stage, *Scx* expression was diminished (Fig. 4B). More posteriorly in wildtype embryos, the two halves of the genioglossus appeared as *Acta2*-positive, wedge-shaped muscle bellies (Fig. 4C). At their ventral aspect, they enclosed two distinct patches expressing *Scx* (Fig. 4C). These tendon primordia were well separated from Meckel's cartilages, and positioned more ventrally. The dorsal tips of the genioglossus halves were seen to reach into the tongue and insert at the *Scx*-positive median fibrous septum. Since all muscle fibers appeared roughly cross-sectioned in frontal sections, they are oriented primarily in the anterior-posterior direction. A very different arrangement was seen in $Bmp7^{\Delta/\Delta}$ embryos at this level: The two genioglossus halves fanned out towards Meckel's cartilages and appeared to be attached to the perichondrium in a broad area expressing *Scx* (Fig. 4D). Image analysis of sections at the medial level showed that the number of *Acta2*-positive fibers per genioglossus half was comparable between E13.5 wildtype (100 ±36), $Bmp7^{+/\Delta}$ (128 ±34) and $Bmp7^{\Delta/\Delta}$ (111 ±14; mean ±SD, n=6) embryos, indicating that Bmp7 does not affect myogenesis per se.

However, many obliquely sectioned genioglossus fibers were visible in *Bmp7*$^{\Delta/\Delta}$ embryos. This indicated that in the mutant, the fibers of this muscle were diverted from the sagittal towards the frontal plane. From a total of seven E13.5-E14.5 *Bmp7*$^{\Delta/\Delta}$ embryos (derived from six independent litters) that were serially sectioned, all exhibited a tongue phenotype as described above.

To support these observations, horizontal sections were prepared through the lower jaws of embryos at E15.5. At a ventral plane, fused Meckel's cartilages were detected in wildtype but not *Bmp7*$^{\Delta/\Delta}$ embryos (Fig. 4E, F). In the wildtype, two oval-shaped *Scx*-positive regions were located just behind the point of fusion of Meckel's cartilages; these are mental spine primordia from which genioglossus fibers originate (Fig. 4E; muscle fibers are not visible because they run caudal-dorsally from this plane.) In contrast, Meckel's cartilages remained unjoined in *Bmp7*$^{\Delta/\Delta}$ embryos and mental spine primordia were missing. Instead, genioglossus fibers were seen to insert laterally into the mandibular periosteum in a *Scx*-positive, aponeurosis-like streak (Fig. 4F). On horizontal sections at a slightly more dorsal plane, the two well-defined bellies of the genioglossus were well separated from the mandibles in the wildtype (Fig. 4G), whereas they irregularly fanned out towards the mandibles in *Bmp7*$^{\Delta/\Delta}$ embryos (Fig. 4H; Supplementary Fig. 2).

In summary, in absence of a rostral process and later a symphysis in *Bmp7*$^{\Delta/\Delta}$ embryos, the anterior attachment of the genioglossus muscle becomes misplaced from the rostral to the lateral aspect of the mandibles, thereby changing the direction of muscle contraction (Fig. 4I, J).

Bmp7 conditional knockout embryos have a mandibular symphysis and no cleft palate

Mice deficient for *Bmp7* only in cranial mesenchyme (*Bmp7*$^{fl/fl}$:Wnt1-Cre) develop to term, but newborns show clear signs of micrognathia (Fig. 5A, B). First signs of shorter snout and lower jaw became visible at E14.5 (Supplementary Fig. 3). E17.5 *Bmp7*$^{fl/fl}$:Wnt1-Cre embryos presented with more slender and slightly shorter mandibles than control littermates, but in contrast to *Bmp7*$^{\Delta/\Delta}$ embryos they had a frontal process (Fig. 5C, D) and did not develop cleft palate (Fig. 5E, F). We therefore examined frontal sections through the lower jaws of such embryos, and found that they did show a developing mandibular symphysis with mental spines (Fig. 5E, F). In more posterior sections of E17.5 *Bmp7*$^{fl/fl}$:Wnt1-Cre lower jaws, the genioglossus halves were clearly separated from the mandibular surfaces, as in wildtype embryos (Fig. 5G, H). Thus, in the two *Bmp7*-deficient mouse strains with various severity of micrognathia, the absence of a frontal process correlates with an overt genioglossus phenotype as well as with palatal clefting, and vice versa. These data also show that epithelial Bmp7 is sufficient for rostral process formation in this case. On the other hand, a

K14-Cre specific Bmp7 deletion has no obvious effect on rostral process and mandible development (D. Graf, unpublished), indicating that mesenchymal Bmp7 can fully compensate for the lack of epithelial.

Discussion

A sequence phenomenon is the widely accepted explanation for palatal clefting in children affected by Pierre Robin syndrome (Price et al. 2015). Several reports on mouse mutants with combined micrognathia and cleft palate assume that obstruction by the tongue due to short mandibles is a causative factor to clefting (Dudas et al. 2004; Murray et al. 2007; Warner et al. 2013). However, how a retrognathic/micrognathic mandible interferes with tongue movement at the stage of palatal shelf elevation is not understood.

This study showed that the rostral process and subsequently the symphysis of Meckel's cartilage do not form in the absence of Bmp7. In consequence, the genioglossus muscle, which mediates tongue protrusion, lacks its physiologic attachment point at the rostral tip, resulting in its lateral diversion towards the lingual surface of the mandibles. The disturbed forward movement of the tongue then interferes with palatal shelf elevation. Our findings provide the best evidence so far that tongue protrusion with a lowering of its dorsal surface is required for freeing the embryonic palatal shelves and spatially allowing their elevation. This is supported by the absence of a palatal cleft in the conditional *Bmp7* knockout mice, in which the genioglossus appears normal although formation of the mandibular bone is affected.

Other models with a Pierre Robin-like phenotype including cleft palate also show altered genioglossus development or orientation. Double mutants for *Hand1/2* transcription factors present with shorter mandibles, hypoplastic genioglossus muscle and cleft palate (Barbosa et al. 2007). Cleft palate also occurs in mouse embryos with defects in tongue muscle proliferation after conditional inactivation of *Tgfbr2* in cranial mesenchyme (Iwata et al. 2013); however, a functional connection between abnormal muscle and cleft palate has not been made. Mice with the same mutation were also shown to have malformed Meckel's cartilage and shorter mandibles (Oka et al. 2007). Interestingly, mouse embryos deficient for *Prdm16*, a transcriptional cofactor of TGF-β signaling, show a similar lateral deflection of genioglossus muscle fibers towards the mandibles around the time of palatal shelf elevation (E14.5), although this has not been pointed out by the authors (Bjork et al. 2010; see their Fig. 1).

Bmps are expressed in the epithelium and mesenchyme of mandibular processes and play a central role during embryonic mandibular osteoinduction (Liu et al. 2005; Merrill et al

2008). Meckel's cartilage is a transient, albeit important structure for intramembranous formation of mandibular bone (Sugito et al. 2011), and there is increasing evidence that Bmps are involved in the growth of both Meckel's cartilage and mandibles (Ekanayake and Hall 1997; Dudas et al. 2004; Liu et al. 2005). It is not understood how Bmp signals regulate the formation of the rostral process and subsequent symphysis of the mandibles. At E13.5 Sox9-positive cells were observed at the tip where the symphysis will form suggesting that a primordium is induced in the absence of Bmp7, but fails to differentiate. It also remains to be investigated whether Bmp7 controls the expression of Scleraxis, a transcription factor essential for tendon development (Schweitzer et al. 2001), and thereby helps to guide genioglossus muscle fibers to their correct origin at the mandibular symphysis. Since neither the mesenchyme- nor the epithelium-specific knockout showed the rostral malformations observed in the null mutant, it is possible that these defects originate from deletion of *Bmp7* in the myogenic lineage (Rot and Kablar 2013).

We conclude that Bmp7 is a necessary factor both for chondrogenesis in Meckel's cartilage and rostral process formation, and its absence leads to altered morphology and stunted development of these structures. In particular, absence of rostral structures leads to disturbances in the attachment sites and the morphology of the genioglossus muscle, which would directly affect the early movements of the tongue, and in *Bmp7* null embryos is the likely cause of cleft secondary palate. These findings help to clear some controversy on the relationship between micrognathia and cleft palate (Price et al., 2015) by pointing to a critical role of genioglossus attachment and movement, rather than of micrognathia *per se*.

Acknowledgements

The authors thank Susan Blumer and Sabrina Ruggiero for expert technical assistance, and Dr. Richard Tucker for critical reading of the manuscript. The senior author would like to dedicate this paper to Dr. Ruth Chiquet-Ehrismann, eminent scientist and invaluable partner and friend over the last 35 years, who sadly and unexpectedly died on September 4, 2015. The authors do not declare any conflicts of interest.

Funding

This work was supported by the Swiss Dental Association (SSO) [grant number 277-13], the Swiss National Science Foundation [grant number 31003A_146825], and by institutional funds from the University of Bern and the University of Alberta.

References

Barbosa AC, Funato N, Chapman S, McKee MD, Richardson JA, Olson EN, Yanagisawa H. 2007. Hand transcription factors cooperatively regulate development of the distal midline mesenchyme. Dev Biol. 310(1):154-168.

d'Amaro R, Scheidegger R, Blumer S, Pazera P, Katsaros C, Graf D, Chiquet M. 2012. Putative functions of extracellular matrix glycoproteins in secondary palate morphogenesis. Front Physiol. 3:377.

Danielian PS, Muccino D, Rowitch DH, Michael SK, McMahon AP. 1998. Modification of gene activity in mouse embryos in utero by a tamoxifen-inducible form of Cre recombinase. Curr Biol. 8(24):1323-1326.

Diewert VM. 1980. Differential changes in cartilage cell proliferation and cell density in the rat craniofacial complex during secondary palate development. Anat Rec. 198(2):219-228.

Fluck M, Tunc-Civelek V, Chiquet M. 2000. Rapid and reciprocal regulation of tenascin-C and tenascin-Y expression by loading of skeletal muscle. J Cell Sci. 113(Pt 20):3583-3591.

Iwata J, Suzuki A, Pelikan RC, Ho TV, Chai Y. 2013. Noncanonical transforming growth factor beta (TGFbeta) signaling in cranial neural crest cells causes tongue muscle developmental defects. J Biol Chem. 288(41):29760-29770.

Kouskoura T, Kozlova A, Alexiou M, Blumer S, Zouvelou V, Katsaros C, Chiquet M, Mitsiadis TA, Graf D. 2013. The etiology of cleft palate formation in BMP7-deficient mice. PLoS One. 8(3):e59463.

Lee YH, Saint-Jeannet JP. 2011. Sox9 function in craniofacial development and disease. Genesis. 49(4):200-208.

Luke DA. 1989. Cell proliferation in palatal processes and Meckel's cartilage during development of the secondary palate in the mouse. J Anat. 165:151-158.

Mina M, Wang YH, Ivanisevic AM, Upholt WB, Rodgers B. 2002. Region- and stage-specific effects of FGFs and BMPs in chick mandibular morphogenesis. Dev Dyn. 223(3):333-352.

Murray SA, Oram KF, Gridley T. 2007. Multiple functions of Snail family genes during palate development in mice. Development. 134(9):1789-1797.

Nonaka K, Shum L, Takahashi I, Takahashi K, Ikura T, Dashner R, Nuckolls GH, Slavkin HC. 1999. Convergence of the BMP and EGF signaling pathways on Smad1 in the regulation of chondrogenesis. Int J Dev Biol. 43(8):795-807.

Oka K, Oka S, Sasaki T, Ito Y, Bringas P, Jr., Nonaka K, Chai Y. 2007. The role of TGF-beta signaling in regulating chondrogenesis and osteogenesis during mandibular development. Dev Biol. 303(1):391-404.

Price KE, Haddad Y, Fakhouri WD. 2015. Analysis of the Relationship Between Micrognathia and Cleft Palate: A Systematic Review. Cleft Palate Craniofac J. [accessed 2015 Feb 6]. http://www.cpcjournal.org/doi/pdf/10.1597/14-238. doi: 10.1597/14-238.

Rot I, Kablar B. 2013. Role of skeletal muscle in palate development. Histol Histopathol. 28(1):1-13.

Schweitzer R, Chyung JH, Murtaugh LC, Brent AE, Rosen V, Olson EN, Lassar A, Tabin CJ. 2001. Analysis of the tendon cell fate using Scleraxis, a specific marker for tendons and ligaments. Development. 128(19):3855-3866.

Sugito H, Shibukawa Y, Kinumatsu T, Yasuda T, Nagayama M, Yamada S, Minugh-Purvis N, Pacifici M, Koyama E. 2011. Ihh signaling regulates mandibular symphysis development and growth. J Dent Res. 90(5):625-631.

Warner DR, Wells JP, Greene RM, Pisano MM. 2013. Gene expression changes in the secondary palate and mandible of Prdm16(-/-) mice. Cell Tissue Res. 351(3):445-452.

Wyatt AW, Osborne RJ, Stewart H, Ragge NK. 2010. Bone morphogenetic protein 7 (BMP7) mutations are associated with variable ocular, brain, ear, palate, and skeletal anomalies. Hum Mutat. 31(7):781-787.

Yu Q, He S, Zeng N, Ma J, Zhang B, Shi B, Jia Z. 2015. BMP7 Gene involved in nonsyndromic orofacial clefts in western han Chinese. Med Oral Patol Oral Cir Bucal. 20(3):e298-304.

Zouvelou V, Luder HU, Mitsiadis TA, Graf D. 2009. Deletion of BMP7 affects the development of bones, teeth, and other ectodermal appendages of the orofacial complex. J Exp Zool B Mol Dev Evol. 312B(4):361-374.

Figure Legends

Figure 1. Impaired Meckel's cartilage development in E12.5-13.5 *Bmp7*$^{\Delta/\Delta}$ embryos. (**A-D**) Whole mounts of embryo heads, stained with Alcian blue for cartilage. On each panel, an individual head is shown in lateral view on the left and in ventral view on the right. Arrowheads point on Meckel's cartilage. (A) *Bmp7*$^{+/+}$, E12.5; (B) *Bmp7*$^{\Delta/\Delta}$, E12.5; (C) *Bmp7*$^{+/+}$, E13.5; (D) *Bmp7*$^{\Delta/\Delta}$, E13.5. Note that the two branches of Meckel's cartilage fail to meet at the midline in E13.5 *Bmp7*$^{\Delta/\Delta}$ embryos. (**E-F**) Anterior frontal sections of wildtype and mutant E12.5 embryo heads, hybridized with probes for cartilage-specific transcription factor Sox9 (*Sox9*) and cartilage collagen type II (*Col2a1*). (E) *Bmp7*$^{+/+}$, (F) *Bmp7*$^{\Delta/\Delta}$. In contrast to nasal cartilage that expresses the two genes in both wildtype and mutant (arrowheads), the frontal process primordium at the midline of the mandible (arrows) appears positive for *Sox9* but not *Co2a1* mRNA in *Bmp7*$^{\Delta/\Delta}$ embryos. p, Palatal shelf; t, tongue. Bar, 2 mm (A-D) or 500 μm (E, F), respectively.

Figure 2. Expression of *Bmp7* and *Bmp4* in mesenchyme and epithelium of the E12.5 mandibular arch. In situ hybridizations were performed with antisense RNA probe specific for *Bmp7* (A-C) or *Bmp4* (D). No staining was observed with a *Bmp7* sense probe on a wildtype section (E), and only a weak signal was detected with *Bmp7* antisense probe on a *Bmp7*$^{\Delta/\Delta}$ section (F). Frontal sections are shown through the anterior (A, D), medial (B, E) or posterior (C, F) part of the mandibular arch. Note that Bmp7 is expressed quite ubiquitously in both epithelium and mesenchyme of the mandibular arch at this stage, with stronger signal in the basal layer of the epidermis and in osteogenic areas of the developing mandibles. e, Epidermis; i, incisor bud; *t*, tongue; *p*, palatal shelf; *m*, Meckel's cartilage; *md*, mandible. Bar, 500 μm.

Figure 3. Lack of a mandibular symphysis formation in *Bmp7*$^{\Delta/\Delta}$ embryos. (**A, B**) Whole mount staining with Alcian blue (cartilage) and Alizarin red (bone) of E17.5 wildtype (A) and *Bmp7*$^{\Delta/\Delta}$ (B) mandibles. Note dented lower lip (arrowhead), lack of rostral process of Meckel's cartilages, and anteriorly blunted mandibles in the mutant (B). Dashed red lines indicate the planes of frontal sections shown in panels E-H, respectively. (C, D) Frontal sections through the secondary palate of E17.5 wildtype (C) and *Bmp7*$^{\Delta/\Delta}$ (D) embryos, hybridized with a probe for *Col1a1* to show bone (blue staining). Note palatal clefting in the mutant (arrowhead in D). (**E-H**) Frontal sections through the anterior mandible of E17.5 wildtype (E, G) and *Bmp7*$^{\Delta/\Delta}$ (F, H) embryos, respectively, at the level of the symphysis (E, F) or slightly more posteriorly (G, H). Sections were hybridized with probes for *Col1a1* (bone),

Acan (cartilage), or *Acta2* (muscle) as indicated. Rostral process and *Acan*-expressing symphyseal cartilage (E; arrowheads) are missing in the *Bmp7*$^{\Delta/\Delta}$ embryo (F). Behind the symphysis, *Col1a1*-positive mental spines are prominent on the medial-ventral surface of wildtype mandibles (G; arrowheads) but absent in the mutant (H). Note also that in the *Bmp7*$^{\Delta/\Delta}$ embryo anterior mandibles are malformed, embedded Meckel's cartilage is barely detectable (H; asterisk), and anterior genioglossus muscle fibers are misplaced (G, H; arrows). *p*, Secondary palate; *t*, tongue; *md*, mandible; *mt*, molar tooth bud; *t*, tongue; *g*, genioglossus muscle; *r*, rostral process; *m*, Meckel's cartilage; *i*, incisor tooth bud. Bar, 800 µm (A, B), 500 (C, D) or 400 µm (E-H), respectively.

Figure 4. Aberrant development of genioglossus muscle attachment sites in *Bmp7*$^{\Delta/\Delta}$ embryos. (**A-D**) Frontal serial sections at an anterior (A, B) or medial level (C, D) through the tongue of E13.5 wildtype (A, C) and *Bmp7*$^{\Delta/\Delta}$ (B, D) embryos, respectively; in situ hybridization for *Acta2* or *Scx* as indicated. Note that in wildtype embryos at this stage, the two genioglossus muscle halves are attached to two Scx-positive tendon primordia that originate from anterior Meckel's cartilage (A) but are separated from it more posteriorly (C). In *Bmp7*$^{\Delta/\Delta}$ embryos, genioglossus tendons do not develop properly (B, D), and the muscle fibers are deflected towards Meckel's cartilage (D). (**E-H**) Horizontal serial sections at a ventral (E, F) or slightly more dorsal level (G, H) through the lower jaw of E15.5 *Bmp7*$^{+/+}$ (E, G) and *Bmp7*$^{\Delta/\Delta}$ (F, H) embryos, respectively, hybridized for *Acta2* or *Scx* as indicated. In the wildtype at this slightly later stage, two oval-shaped Scx-positive areas are visible just behind the fusion of Meckel's cartilages (E, arrows). These are mental spine primordia to which the genioglossus attaches. More dorsally (G), the two genioglossus bellies are well separated from the mandibles and contain Scx-positive tendons (arrows). In the mutant, Meckel's cartilages remain unfused (F), and genioglossus muscle fibers fan out towards the mandibles, where they attach in a broad Scx-positive aponeurosis (F, G; arrowheads). (I, J) Schemes of genioglossus attachments in wildtype and *Bmp7*$^{\Delta/\Delta}$ embryos. In the wildtype (I), genioglossus fibers (red) arise from two focused tendon insertions (brown) on Meckel's cartilages (blue) just posteriorly from the rostral process; these later become the mental spines of mandibles. In the mutant (J), rostral structures are missing, and genioglossus fibers attach laterally to Meckel's cartilages and later mandibles (not drawn). This causes a change in the direction of movement of the tongue (beige) from rostrally to ventrally (arrows). *t*, Tongue; *m*, Meckel's cartilage; *r*, rostral process; *g*, genioglossus muscle; *tn*, tendon primordia; *md*, mandible. Bar, 500 µm (800 µm in *Acta2* panels of E-H).

Figure 5. Mice with a conditional deletion of Bmp7 in cranial mesenchyme (*Bmp7*$^{fl/fl}$:Wnt1-Cre) show signs of micrognathia, but have a mandibular symphysis, an apparently normal

genioglossus muscle, and no cleft palate. **(A, B)** Micro-CT images of the skulls of newborn *Bmp7*$^{fl/fl}$ control (A) and *Bmp7*$^{fl/fl}$:Wnt1-Cre mice, respectively. Note shorter skull, maxillae and mandibles in the mutant. **(C, D)** Whole mount staining of E17.5 *Bmp7*$^{fl/fl}$ control (C) and *Bmp7*$^{fl/fl}$:Wnt1-Cre (D) mandibles with Alcian blue and Alizarin red. Note the presence of a rostral process in both the control and the mutant embryo. **(E-J)** Frontal sections depicting the palate and mandibles (E, F), the genioglossus muscle (G, H), and the mandibular symphysis (I, J) of E17.5 *Bmp7*$^{fl/fl}$ control (E, G, I) and *Bmp7*$^{fl/fl}$:Wnt1-Cre (F, H, J) embryos, respectively. Sections were hybridized with RNA probes for *Col1a1* (E, F, I, J) or *Acta2* (G, H). Note the absence of a cleft palate (H), a normal genioglossus muscle (H), and the presence of a symphysis (J) in the mutant. *m*, Meckel's cartilage; *md*, mandible; *r*, rostral process; p, palate; t, tongue; tn, genioglossus tendon; *g*, genioglossus muscle. Bar, 0.5 cm (A, B); 800 μm (C, D); 500 μm (E-F), 300 μm (I, J).

Fig. 1

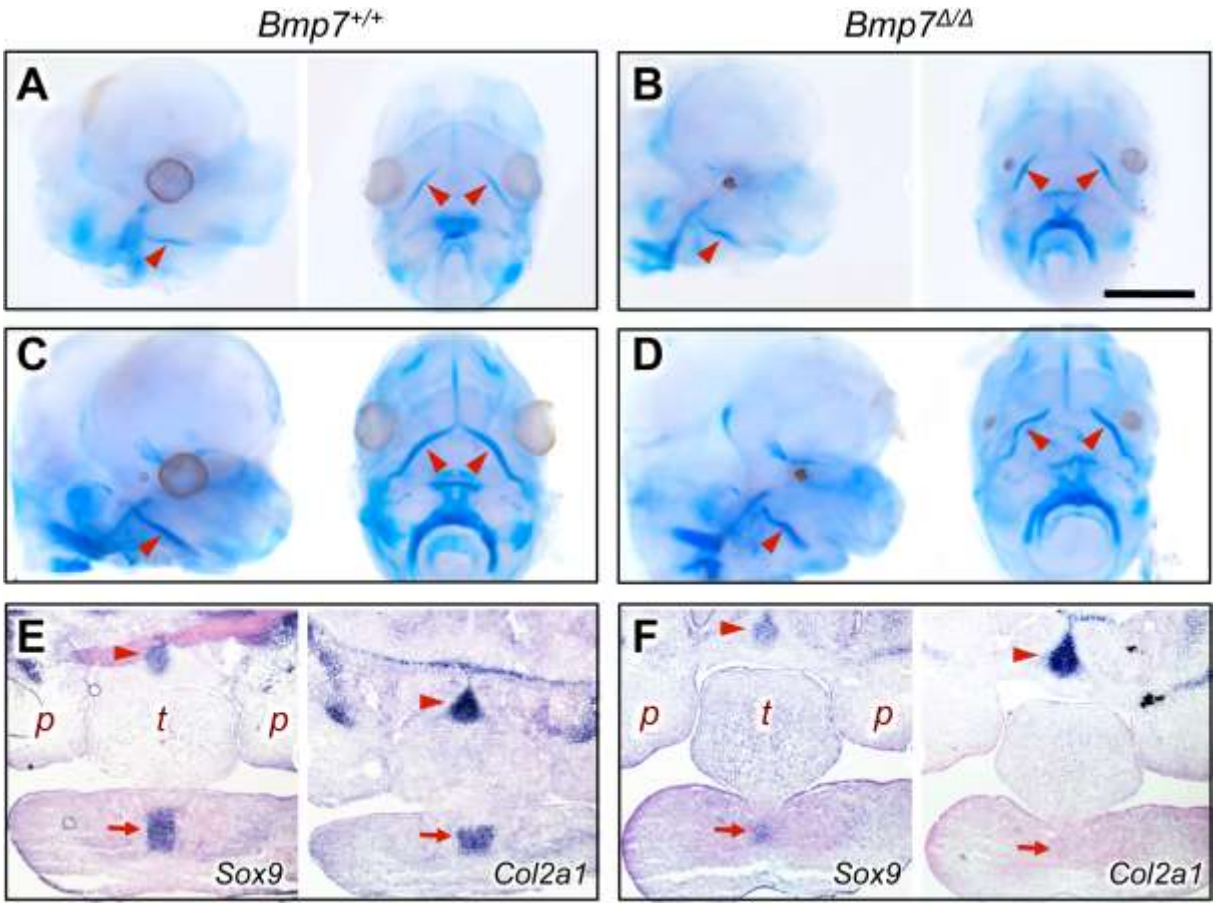

Fig. 2

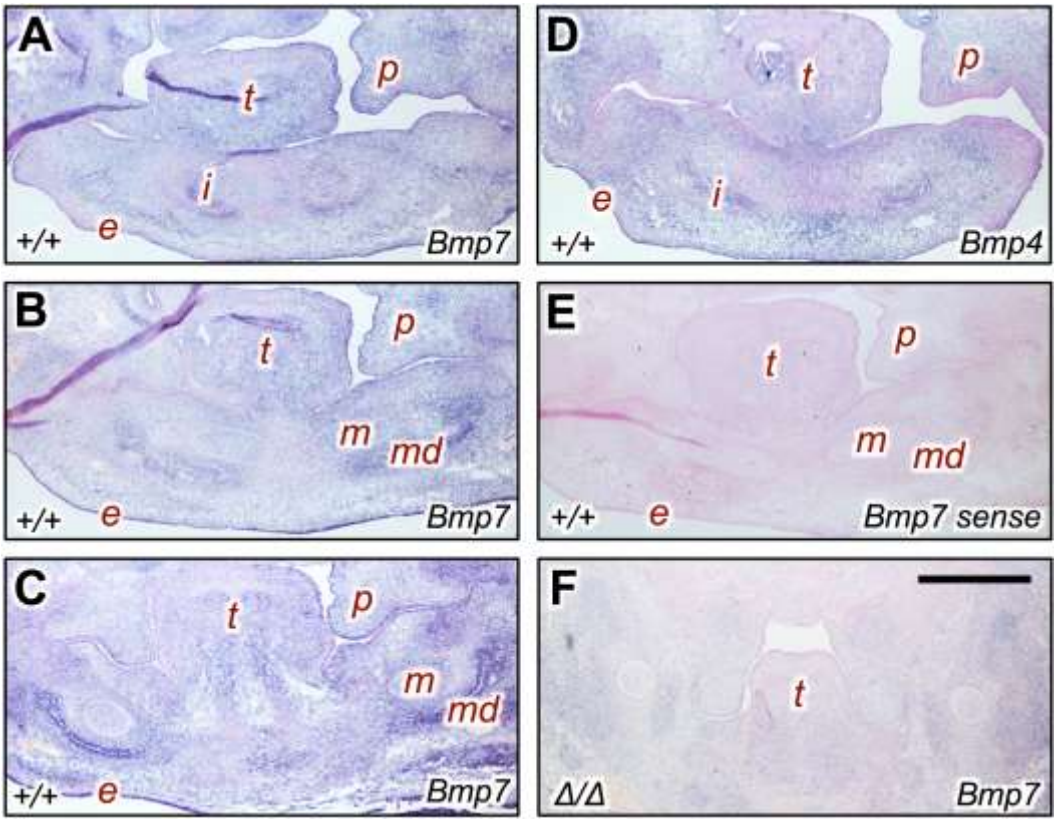
A
t
p
i
e
+/+
Bmp7
D
t
p
e
i
+/+
Bmp4
B
t
p
m
md
+/+
e
Bmp7
E
t
p
m
md
+/+
e
Bmp7 sense
C
t
p
m
md
+/+
e
Bmp7
F
t
Δ/Δ
Bmp7

Fig. 3

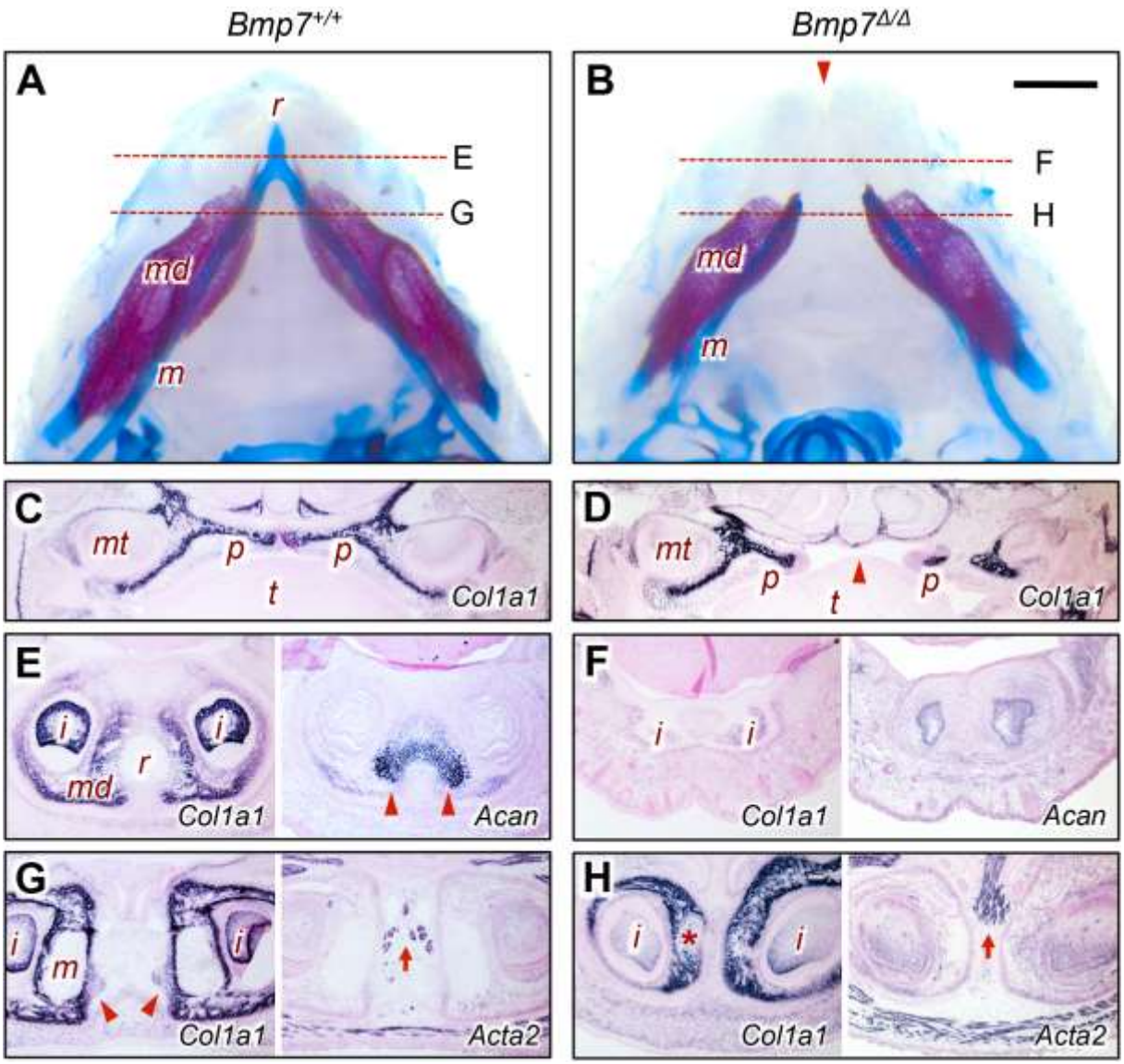
Bmp7+/+
Bmp7Δ/Δ
A
r
E
G
md
m
B
F
H
md
m
C
mt
p
p
t
Col1a1
D
mt
p
t
p
Col1a1
E
i
i
r
md
Col1a1
Acan
F
i
i
Col1a1
Acan
G
i
m
i
Col1a1
Acta2
H
i
*
i
Col1a1
Acta2

Fig. 4

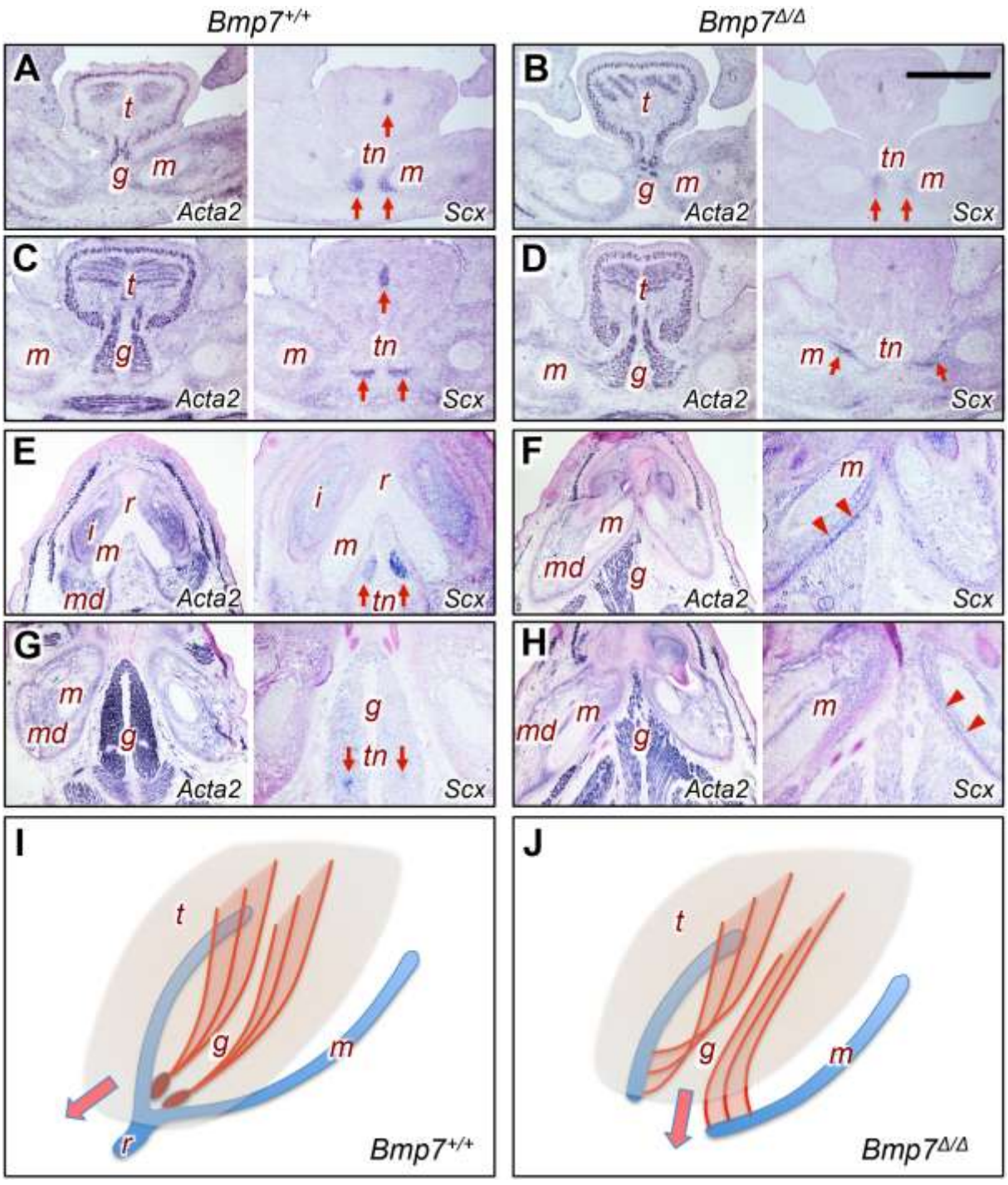
Bmp7+/+
Bmp7Δ/Δ
A
t
g
m
Acta2
tn
m
Scx
B
t
g
m
Acta2
tn
m
Scx
C
t
m
g
Acta2
m
tn
Scx
D
t
m
g
Acta2
m
tn
Scx
E
r
i
m
md
Acta2
i
r
m
tn
Scx
F
m
md
g
Acta2
m
Scx
G
m
md
g
Acta2
g
tn
Scx
H
md
m
g
Acta2
m
Scx
I
t
g
m
r
Bmp7+/+
J
t
g
m
Bmp7Δ/Δ

Fig. 5

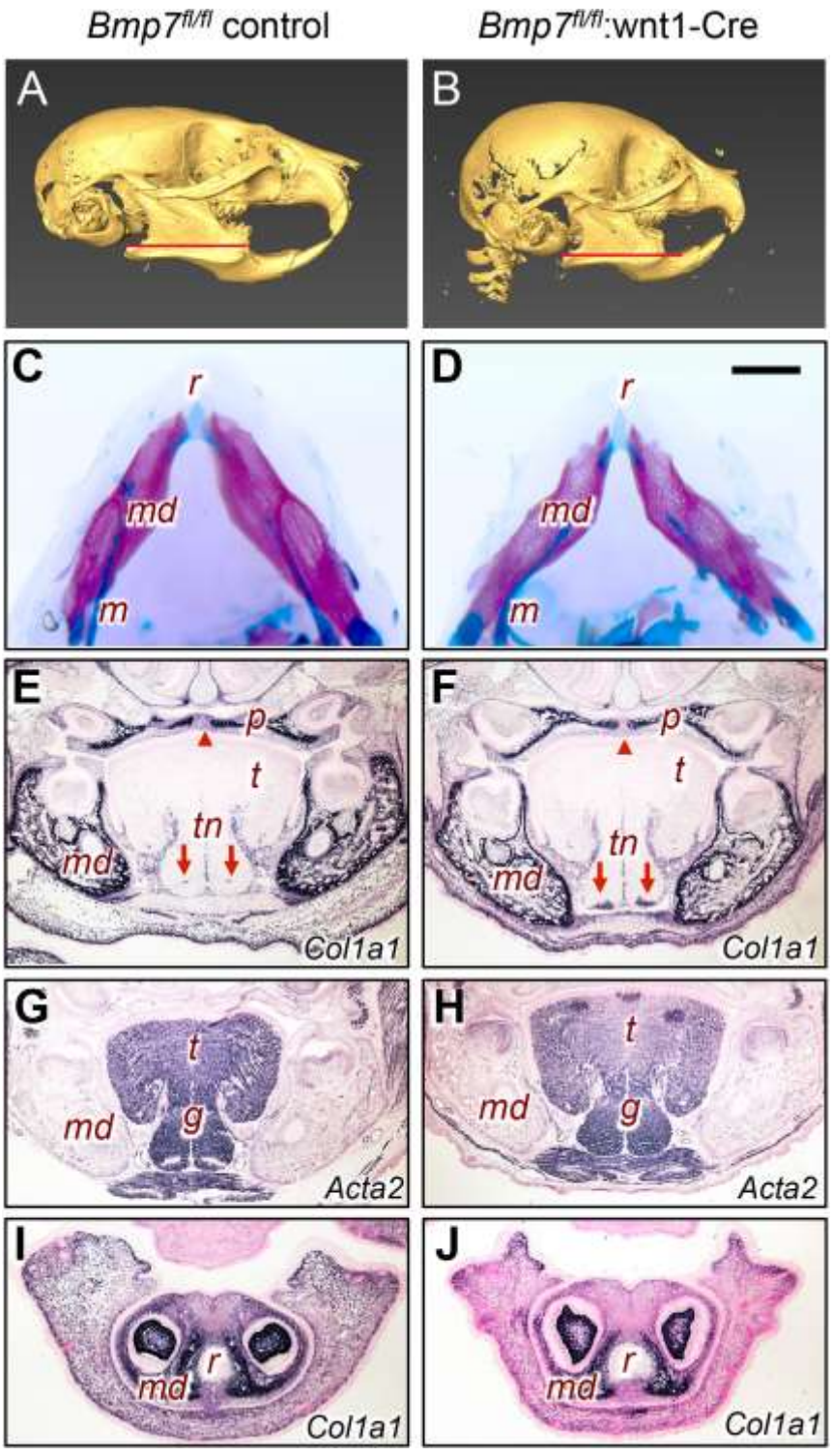
Bmp7fl/fl control
Bmp7fl/fl:wnt1-Cre
A
B
C
r
md
m
D
r
md
m
E
p
t
tn
md
Col1a1
F
p
t
tn
md
Col1a1
G
t
md
g
Acta2
H
t
md
g
Acta2
I
r
md
Col1a1
J
r
md
Col1a1

Gene	Forward Primer	Reverse Primer
Acan	CCGGATCCTGTGTACTGCTTCGCTGAGG	CCAAGCTTGAATACAACTCCCCCTGGCA
Acta2	CCGGATCCTGGCCCCTGAAGAGCATCCG	CCAAGCTTGCCCGCTGACTCCATCCCA
Col1a1	CCGGATCCCCAATGGTGAGACGTGGAA	CCAAGCTTGGACCCATTGGACCTGAACC
Col2a1	CCGGATCCACTGGGAATGTCCTCTGCGA	CCAAGCTTCTCTGTGACCCTTGACACCG
Sox9	CCGGATCCGGGCGAGCACTCTGGGCAA	CCAAGCTTCGCTGTAGTGGCTGGGGCT

Supplemental Table 1: Primers used for amplifying cDNAs specific for mouse genes. Products were cloned into Bluescript vector, and digoxygenin-labeled RNA probes were generated for in situ hybridization as described in Materials and Methods.

Supplementary Figure 1 Kouskoura et al.

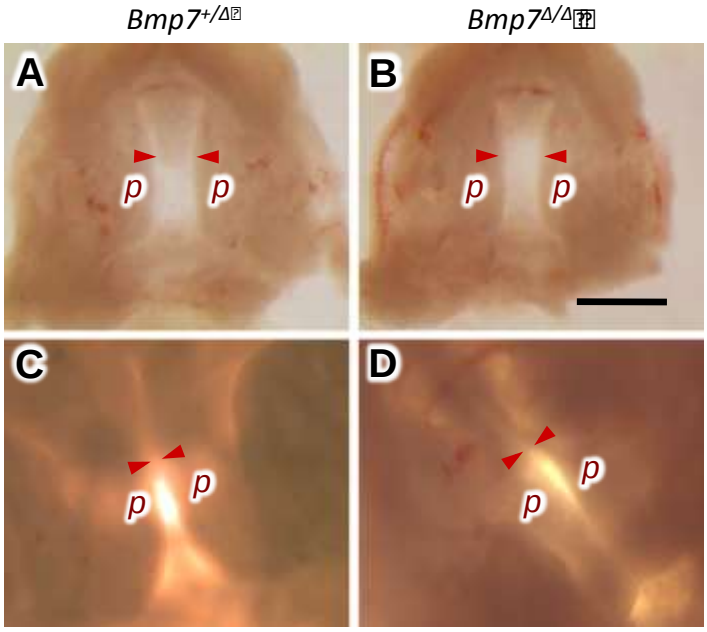

Supplementary Fig. 1. E13.5 *Bmp7*$^{\Delta/\Delta}$ palatal shelves are able to elevate and meet at the midline when cultured in the absence of mandibles and tongue. (**A-D**) Maxillae with attached palatal shelves were microdissected from E13.5 heterozygous *Bmp7*$^{+/\Delta}$ (A, C) and knockout *Bmp7*$^{\Delta/\Delta}$ (B, D) embryos and cultured as described below. Photographs of the explants were taken from ventrally immediately after microdissection (A, B) and at higher magnification after 15 h of culture (C, D); anterior is up. Arrowheads point to the medial edge epithelia of palatal shelves (p) before (A, B) and after closure of the cleft (C, D). Bar, 200 μm (A, B) or 100 μm (C, D), respectively.

Methods: *Bmp7*$^{+/+}$, *Bmp7*$^{+/\Delta}$ and *Bmp7*$^{\Delta/\Delta}$ embryo heads were collected at E13.5, and brain, mandibles and tongue were removed. Each maxillary region with attached palatal shelves was cultured in a 50 ml tube mounted on a roller bottle system (Fisher Scientific, Reinach, Switzerland; 22 rpm) for 24-48 hours in 5 ml serum- and protein-free BGJb medium (Yumoto et al. 2013) (Life Technologies, Lucerne, Switzerland). The medium was bubbled with 90% O_2, 10% CO_2 every 12 hours. Explants were photographed at indicated time points.

Supplementary Figure 2 Kouskoura et al.

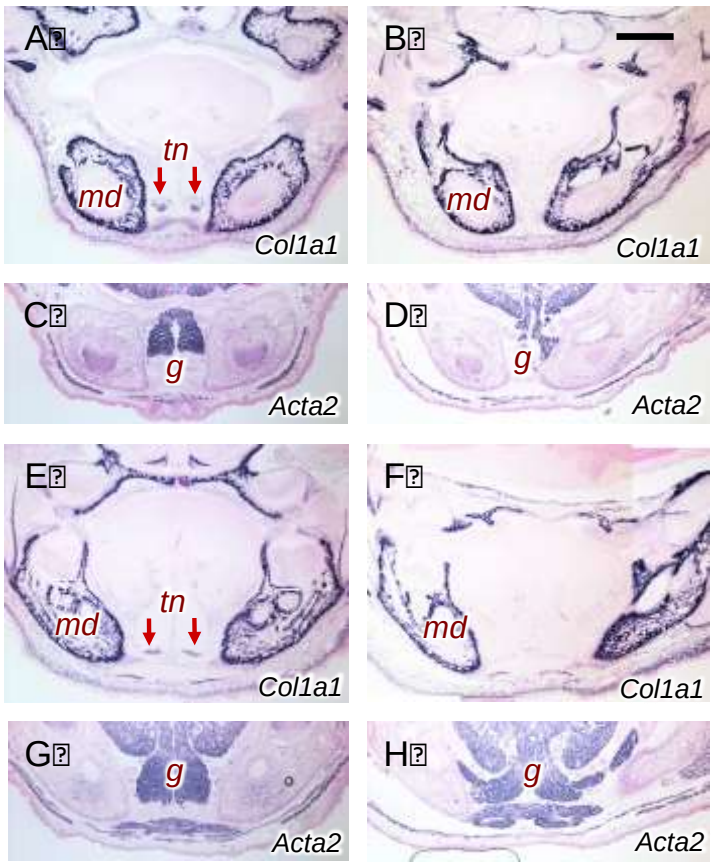

Supplementary Fig. 2. Frontal sections at an anterior (A-D) and a medial (E-H) level through the heads of E17.5 *Bmp7*$^{+/+}$ (A,C,E,G) and *Bmp7*$^{\Delta/\Delta}$ (B,D, F, H) embryos, respectively. Sections were hybridized for *Col1a1* (A, B, E, F) or *Acta2* (C, D, G, H). Note deviation of genioglossus fibers towards the mandibles and absence ofgenioglossus tendons in the mutant. md, Mandibles; tn, genioglossus tendons; g, genioglossus muscle. Bar, 500 μm.

Methods: See Materials and Methods.

Supplementary Figure 3 Kouskoura et al.

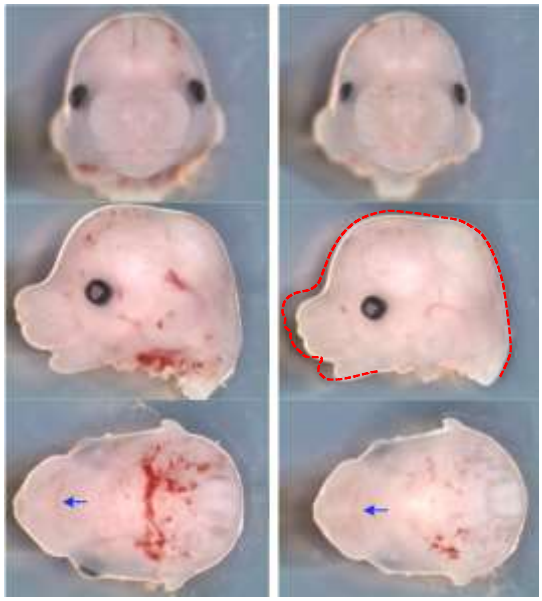

Supplementary Fig. 3. Heads of E14 Bmp7fl/fl and Bmp7:wnt1-Cre embryos. Note shorter snout and a shorter and less pointed (arrows) lower jaw in the mutant.